Materials Research. 2016; 19(5): 999-1007
DOI: http://dx.doi.org/10.1590/1980-5373-MR-2015-0502

Polypyrrole/Metal Sulphide Hybrid Nanocomposites: Synthesis, Characterization and Room Temperature Gas Sensing Properties

Bharti Yeole[a], Tanushree Sen[a], Dharmesh Hansora[a], Satyendra Mishra[a]*

[a]Department of Plastic Technology, University Institute of Chemical Technology, North Maharashtra University, Jalgaon 425001, Maharashtra, India

Received: August 26, 2015; Revised: March 9, 2016; Accepted: July 8, 2016

The present research work explores the room temperature gas sensing ability of hybrid nanocomposites of metal sulphide nanoparticles with polypyrrole (PPy) matrix. Sonochemically synthesized both silver sulphide (Ag_2S) and cadmium sulphide (CdS) nanoparticles were mixed in varying ratios with PPy matrix by *in-situ* oxidative polymerization route. The resulting PPy/(Ag_2S:CdS) hybrid nanocomposites were analyzed by characterizing them using FTIR and UV-Visible spectroscopy, XRD, SEM, four-probe conductivity method and gas sensing ability by two-probe gas sensing setup. The current-voltage (I-V) characteristics of the PPy hybrid nanocomposites revealed their semiconducting nature with an electrical conductivity in the range of 10^{-4} to 10^{-3} S/cm. As compared to pure PPy, their hybrid PPy/(Ag_2S:CdS) nanocomposites showed an enhancement in sensitivity towards ammonia gas detection. The results clearly indicated a synergistic effect between the Ag_2S:CdS nanoparticles and the PPy matrix.

Keywords: *Metal sulphide nanoparticles, Hybrids, Polypyrrole, Gas sensing*

1. Introduction

Various nanomaterials and nanofillers have been tested for the preparation of polymer nanocomposites.[1-7] Over the decade, there has been a steady progress in the applications of conjugated conducting polymers (CPs) such as in chemical sensors, electrochemical supercapacitors, electro chromic and photovoltaic devices, light-emitting diodes and batteries. The years in the last decade have also witnessed consistent efforts by researchers in improving the physical and structural properties of CPs.[1,5-12] The physical and structural attributes of CPs are generally affected by crucial parameters such as polymerization method, type of the oxidant, pH and temperature conditions during polymerization, etc. In recent times, however, tuning of CPs' properties has also been attempted by use of nanomaterials. Selection of appropriate nanomaterial for a CP is crucial to the ultimate application of the resulting nanocomposites, which is generally a result of the synergistic effect between the CP and the nanomaterial.[5,7,12-14] Using nanotechnology, various macromolecules and nanomaterials have been used for gas sensing purposes[15,16] and amongst them metal oxides[17,18] and CPs[19] are most widely used. A silver nanocrystal has been reported as a promoter for carbon nanotube-based gas sensors at room-temperature.[20] Silver sulphide (Ag_2S) is semiconducting filler, which can be used in preparation of photo electrochemical devices and solar cells. Polymers encapsulated with metal nanocrystal can be used as a promoter for room-temperature gas sensors.[11] Polypyrrole (PPy) is a promising candidate among the CPs because of its good chemical and environmental stability, high electrical conductivity and ease of synthesis.[7-9,21-23] Bulk production of PPy is also possible by oxidative polymerization of pyrrole in aqueous or non-aqueous media. Various methods and routes have been successfully used to prepare PPy and their nanostructures.[7,21-23] Various metals, metal oxides and metal sulphide nanoparticles have been incorporated in PPy matrix and the resulting CP nanocomposites showed an improvement in their properties. In particular, these nanocomposites have shown much promise as sensors for a range of analytes.[24-26]

Amongst the various toxic gases, ammonia (NH_3) gas is particularly lethal for humans as well as land and aquatic animals over 500 ppm concentration. NH_3 is commonly present in fertilizers, household cleaners and in compressors of air conditioner. It is also an important component of industrial production of synthetic polymers and explosives. It is highly toxic with a permissible exposure limit of 25 ppm for human beings and forms an explosive mixture with air at ~16-25%. These reasons make necessary the detection of NH_3 gas at room temperature. Researchers have also developed sensors based on various polymers, metal sulphides[7], metal oxides [26-28] and their composites[29], which can be used to detect NH_3 gas. But, it is more important to develop sensors that should be cheap and small in size and can be operated at room temperature.

In this study, we investigate the possibility of PPy/silver sulphide: cadmium sulphide nanoparticles (Ag_2S:CdS) based hybrid nanocomposites as gas sensors for detection of ammonia (NH_3) gas. The PPy/(Ag_2S:CdS) hybrid nanocomposites were characterized using FTIR and UV-Visible spectroscopy, XRD and SEM. We also report the effect of composition (varying

---

* e-mail: profsm@rediffmail.com

amounts of Ag_2S:CdS nanoparticles) on the structural, morphological, electrical and sensing properties of the hybrid nanocomposites (PPy/Ag_2S:CdS). The sensing performance of the PPy based hybrid nanocomposites towards detection of ammonia and LPG was investigated at room temperature and the results are discussed in detail.

2. Experimental

2.1. *Materials*

Analytical grade pyrrole and anhydrous ferric chloride ($FeCl_3$) were purchased from Merck (Mumbai, India). Sodium lauryl sulphate (SLS) and silver nitrate ($AgNO_3$) were received from S.D. Fine Chem. Ltd. (Mumbai, India). Cadmium nitrate ($CdNO_3$) was received from Loba Chemie Ltd. (Mumbai, India), while sodium sulphide (Na_2S) was received from Himedia Laboratories Pvt. Ltd. (Mumbai, India). Ultra-pure water was prepared by Smart 2 Pure system (Thermo Electron LED GmbH, Germany) and then used for preparing solutions, cleaning as well as washing purposes. Acetone and methanol were received from S.D. Fine Chem. Ltd. (Mumbai, India) and were used for washing purposes. Ammonia and LPG (99.9% purity) gases were purchased from Master Specialty Gases Pvt. Ltd. (Mumbai, India). Microscope glass slides were purchased from the Polar India Corporation, (Mumbai, India) and used for deposition of films of PPy and its hybrid nanocomposites.

2.2. *Sonochemical synthesis of metal sulphide nanoparticles*

Sonochemical synthesis of both Ag_2S and CdS nanoparticles was carried out as per our previous work.[7] In brief, aqueous solution of Na_2S was added drop-wise to an aqueous solution of $AgNO_3$ or $Cd(NO_3)_2$ under ultrasound (BO3 Ultrasonic Processor UP1200, Cromtech, India) at room temperature (30 ± 2 °C). Both metal sulphide nanoparticles were obtained in the precipitate form at the end of the reaction, which were centrifuged at 8000 rpm, washed with acetone and then finally with water. These metal sulphide nanoparticles were then allowed to dry in air at temperature of 60 °C. During the reactions involved in the sonochemical synthesis, the metal nitrates get converted into metal sulphides.

2.3. *Synthesis of PPy and their nanocomposites*

Films of PPy were prepared by oxidative polymerization (as per our previous work[7]) using $FeCl_3$ as the oxidant. A solution of 0.2M of pyrrole and 0.466 M of $FeCl_3$ was prepared in 100 mL distilled water by keeping monomer to oxidant ($FeCl_3$ to pyrrole) molar ratio to be (1:2.33). A solution of 0.2M pyrrole was stirred continuously on magnetic stirrer at 400 rpm and simultaneously 0.466M $FeCl_3$ was added drop wise by keeping rate of one drop per second, simultaneously induction time was noted. The reaction was allowed to proceed for 2 h and then left to stand overnight. Films of PPy were deposited on microscope glass slides during the polymerization of pyrrole. At the end of polymerization reaction, the glass slides were taken out of the reaction mixture, sequentially washed with water and ethanol and then dried under vacuum. The black precipitate of PPy was repeatedly washed with water and acetone and then dried at room temperature.

For the preparation of PPy hybrid nanocomposites, predetermined weight ratios of Ag_2S and CdS nanoparticles were dispersed into the pyrrole solution by ultrasound treatment and then pyrrole was polymerized as per the procedure mentioned above. Different compositions of PPy/(Ag_2S:CdS) nanocomposites were prepared and deposited on glass slides, wherein the Ag_2S:CdS nanoparticles were taken in different ratios, viz., 1:1, 2:1 and 1:2, and are henceforth labelled as AC1, AC2 and AC3, respectively. The glass slides for thin film deposition of PPy and its hybrid nanocomposites were cleaned. These slides were cleaned by completely immersing them in 0.1M HCl solution for 1 h and then successively sonicated in water bath and methanol for 15 min each followed by vacuum drying.

2.4. *Preparation of pellets*

To measure electrical conductivity and gas sensing performance, the pellets (diameter of 10 mm and 2 mm thick) of PPy and its hybrid nanocomposites were prepared in a Hydraulic Press Machine, Kimaya Engineering (Mumbai, India). A 0.2 mg of sample was taken between two die plates and pressurized by the hydraulic press to obtain pellets having a diameter of 15 mm.

2.5. *Characterizations*

Powder form of pristine PPy and PPy/(Ag_2S:CdS) hybrid nanocomposites were prepared by mixing with potassium bromide (KBr) and their FTIR spectra was recorded on Shimadzu FTIR-8400 spectrophotometer (Tokyo, Japan) within the wavenumber range of 400–4000 cm^{-1}. UV–visible absorption spectra of pristine PPy and PPy/(Ag_2S:CdS) nanocomposites taken in dimethyl formamide (DMF) on a Hitachi U-2900 spectrophotometer (Tokyo, Japan) in the range of 200–800 nm. Blank DMF (without reactants) was used as reference in UV spectrophotometer. The excitation wavelength was 800 nm and slit width was taken as 10 nm for excitation and emission. UV spectra were obtained from the quartz cuvettes filled solution of different PPy hybrid nanocomposites and DMF. X-ray diffraction (XRD) analysis of pristine PPy and PPy/(Ag_2S:CdS) nanocomposites (AC1, AC2 and AC3) were carried out by Advance X-ray diffractometer (Brukers D8, Germany) with CuKα1 radiation (λ = 1.5404 Å). The surface morphology of PPy and PPy/(Ag_2S:CdS) nanocomposites films was observed in a field emission scanning electron microscope (Hitachi S-4800, Tokyo, Japan) by mounting samples on a specimen stub. The electrical conductivity of various composites was measured by four-point probe conductivity method, using a current source (CCS-01) and a micro voltmeter (DMV-001, SES Instruments, Scientific Equipments, Roorkee, India). The resistance of the nanocomposite sensors was measured with a programmable 4.5 digital multimeter (SM 5015, Scientific MES-Technik Private Limited, Indore, India) connected to a computer (QT035AV, Hewlett Packard, Banglore, India) using a RS232C interface that was fully automated and logged by a program. Current-Voltage (I–V) characteristics of the all pellets were recorded in the bias range of 0.15 to −0.15 V and the electrical conductivity of the films was deduced from the plot of Current-Voltage (I–V) graphs. Pellets of PPy and PPy/(Ag_2S:CdS) nanocomposites (AC1, AC2 and AC3) were loaded into a sensing chamber (Figure 1) and two conducting probes were placed in contact with the pellets. The sensor response was measured from current-time characteristics of each sample recorded first in ambient air and then in different concentration (100, 250 and 500 ppm) of NH_3 and LPG gases. All electrical data were recorded at room temperature (30 ± 2 °C). The response factor of the sensor was measured from the change in electrical current observed in presence and absence of testing gas using the following Eq. (1), in which, I_a is current measured in the presence of air and I_g is current measured in the presence of testing gas.

$$Gas\ Response = \left(\frac{I_a - I_g}{I_a}\right) \quad (1)$$

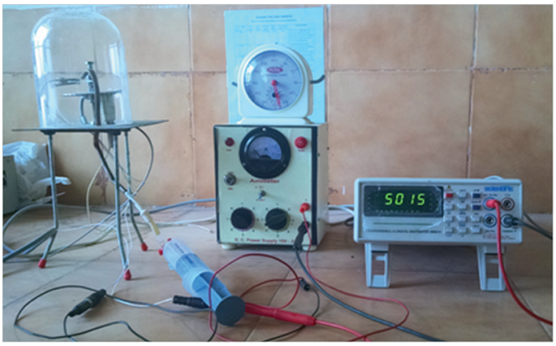

Figure 1. Photographic view of gas sensing setup.

3. Results and Discussion

3.1. *Oxidative polymerization mechanism*

PPy and PPy/(Ag_2S:CdS) nanocomposites were prepared (as per our previous work[7]) by an oxidative polymerization method at room temperature. The first step in the polymerization reaction is the oxidation of Fe^{3+} ion to give pyrrole radical cation. This is followed by dimerization of the radical cations with expulsion of two protons. The chain propagation occurs through the addition of a new radical cation. The preparation of nanocomposites, as shown in Figure 2, involves the attachment of the hydrophobic oligomeric units of pyrrole on the nanoparticle surface. These nanoparticles serve as a nucleation site for the polymer. As polymerization proceeds, the both nanoparticles get embedded into the polymer matrix resulting in the formation of hybrid nanocomposites. The use of ultrasound facilitates uniform dispersion of the nanoparticles in the monomer solution during polymerization, which is crucial for the better performance of a nanocomposite.

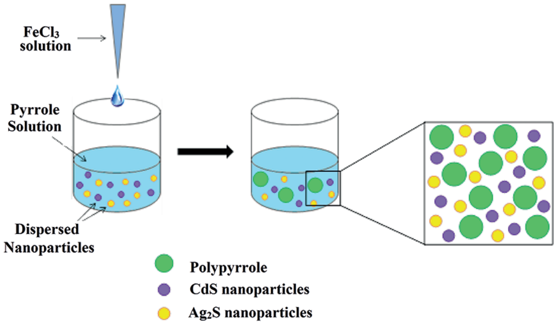

Figure 2. Chemical oxidative polymerization of PPy/(Ag_2S:CdS) hybrid nanocomposites.

3.2. *FTIR spectra*

Figure 3 shows the FTIR spectra of PPy and PPy/(Ag_2S:CdS) nanocomposites. A peak near around 467 cm^{-1} in the spectra of the all PPy nanocomposites is associated with Ag_2S nanoparticles. The spectra of PPy hybrid nanocomposites (AC1, AC2 and AC3) show slightly shifted peaks: band at 1043 cm^{-1} shifted to 1045 cm^{-1} due to the N-H in-plane deformation[10,12] caused by interaction between Ag_2S:CdS nanoparticles and PPy matrix. The peak at 1375 cm^{-1} is related to the asymmetric C-H stretching in the PPy ring, while 778 cm^{-1} is due to the plane deformation of C-N in PPy[9]. The characteristic peaks for pristine PPy can be observed at 1542 and 1466 cm^{-1} that are related to the fundamental vibrations of pyrrole ring.[7,12] The peak at 2928 cm^{-1} associated with C-H vibrations. The broad region at about 3400 cm^{-1} refers to vibrations of N-H stretching.[10,12] These results indicated that the extent of oxidation of PPy increased by increasing the molar ratio of the oxidant and the monomer.

3.3. *UV spectra*

The UV–visible spectra of PPy and PPy/(Ag_2S:CdS) nanocomposites is shown in Figure 4. The UV–visible spectroscopy indicates the presence of Ag_2S and CdS nanoparticles, which led to UV light absorption at different wavelengths. Pristine PPy shows weaker absorption ~ 270 nm due to π electron system present in PPy matrix. This band is

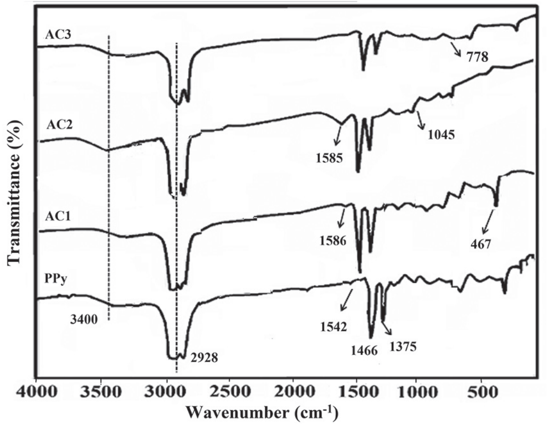

Figure 3. FTIR spectra of PPy and PPy/(Ag_2S:CdS) hybrid nanocomposites.

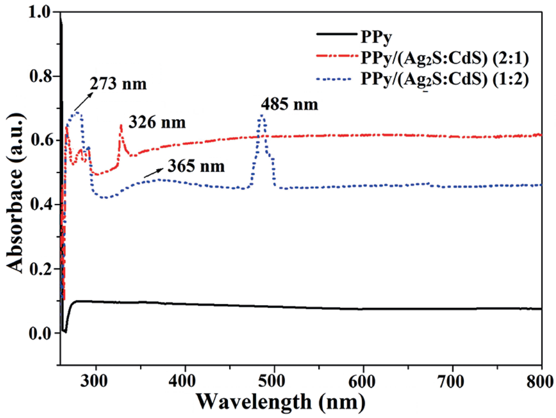

Figure 4. UV-visible spectra of PPy and PPy/(Ag_2S:CdS) nanocomposites.

observed at ~ 273-275 nm in AC1 and AC3 nanocomposites. The shift in peaks in the spectrum indicates interaction of Ag_2S and CdS nanoparticles with PPy chains in the AC3 hybrid nanocomposites. The peak at 650 cm^{-1} shows the slight stretching of CdS in AC3 hybrid nanocomposites, while for Ag_2S metal stretching band appears at 467-487 cm^{-1} in AC1 hybrid nanocomposites.[7] No obvious absorbance for Ag_2S and CdS nanoparticles was observed in the spectra of AC1 hybrid nanocomposites due to the agglomeration of the both nanoparticles, which might have affected the UV visible absorption spectrum. Since the interaction of PPy with solvent molecules may be very low, hence its corresponding absorption could be absent in the spectra. The peak may shift towards higher energy that accounts to reduce the PPy after addition of NPs[12]. The absorption peak at $\lambda > 300$ nm is possibly due to interaction of the polymer with the solvent.

3.4. *Crystallinity*

In Figure 5 (a), XRD pattern of PPy shows amorphous nature and a broad diffraction peak at 25°, which is associated with (1 1 2) plane[7,12]. The peaks observed for Ag_2S nanoparticles are in the planes (1 1 1), (1 2 0), (0 2 2), (1 1 2) and (0 3 1) corresponding to the d-values 3.08, 2.6, 2.58, 2.45 and 2.21 nm, respectively. The crystallite size of these Ag_2S nanoparticles was recorded as ~ 61 nm, while their crystallinity was ~70.6 %. An additional diffraction peaks near 27 °, 31 ° and 46 ° are associated with (0 1 2), (1 2 0) and (2 2 1) planes of Ag_2S nanoparticles, respectively. For the CdS nanoparticles, the observed peaks have d-values 3.3, 2.8, 2.0, 1.7 and 1.65 nm corresponding to (1 1 1), (2 0 0), (2 2 0), (3 1 1) and (2 2 2) planes, respectively. The crystallite size of the CdS nanoparticles was recorded as 84 nm and the crystallinity was ~38.6 % [7]. Figure 5 (b) shows XRD spectra of the PPy hybrid nanocomposites (AC1, AC2 and AC3). In addition to the characteristic peak of PPy, peaks related to Ag_2S and CdS are also clearly observed. This confirms the presence of Ag_2S and CdS nanoparticles in the PPy based hybrid nanocomposites. It was observed that the crystallinity of the PPy based hybrid nanocomposites decreases with increase in CdS nanoparticles content: which can be confirmed from crystallinity of AC1, AC2 and AC3 hybrid nanocomposites was recorded as 49.6, 47 and 38.2 %, respectively. On the other hand, higher amount of Ag_2S nanoparticles in PPy based hybrid nanocomposites exhibited a greater crystallinity.

3.5. *Surface morphology and elemental analysis*

PPy has a globular[7,12] and porous[10] morphology, which can be confirmed from Figure 6 (a-b). Uniform, nanospheres of Ag_2S particles have diameter of ~ 40-65 nm (Figure 6 (c)), while CdS nanoparticles possess diameter of ~ 60-100 nm can be seen from Figure 6 (d). This indicates the effectiveness of ultrasound in producing non-aggregated nanoparticles even in the absence of an encapsulating agent. The morphology of PPy/(Ag_2S:CdS) hybrid nanocomposites (AC2) can be observed to be spherical as shown in Figure 6 (e). It is evident from the FE-SEM micrographs that ultrasound assisted *in-situ* polymerization can produce non-aggregated structures of PPy matrix.

Figure 7 (a-b) shows the energy dispersive X-ray (EDX) spectra of AC1 and AC2 nanocomposites. The EDX result confirmed that the PPy hybrid nanocomposites were properly embedded metal sulphide nanoparticles. It can be also observed from FE-SEM micrographs in Figure 6 (c-d) that two metal sulphide nanoparticles are uniformly dispersed in PPy matrix. Elements like carbon (C) and nitrogen (N) are observed due to the presence of pyrrole, while other elements such as silver (Ag), cadmium (Cd) and sulphur (S) are due to the presence of metal sulphide nanoparticles and their proper dispersion in PPy matrix. The EDX spectrum (Figure 7 (a)) of AC2 nanocomposites showed Ag, Cd, S, N and C peaks, which indicates the wt% composition (C = 34.08, N = 15, Ag = 1.91, Cd = 0.33 and S = 0.7 wt%).

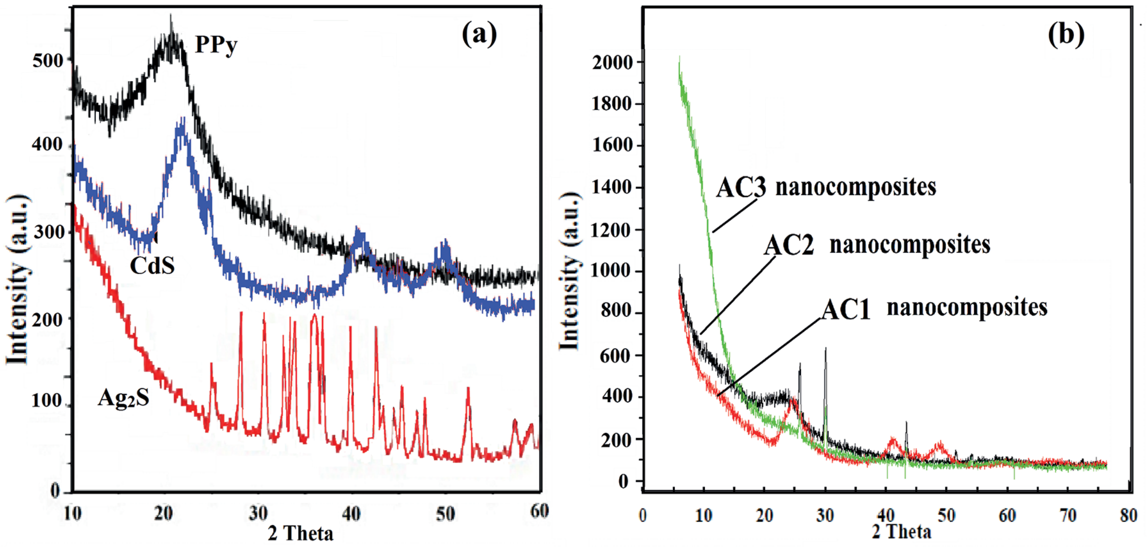

Figure 5. X-ray diffractograms of (a) pristine PPy, Ag_2S and CdS nanoparticles and (b) PPy/(Ag2S:CdS) hybrid nanocomposites.

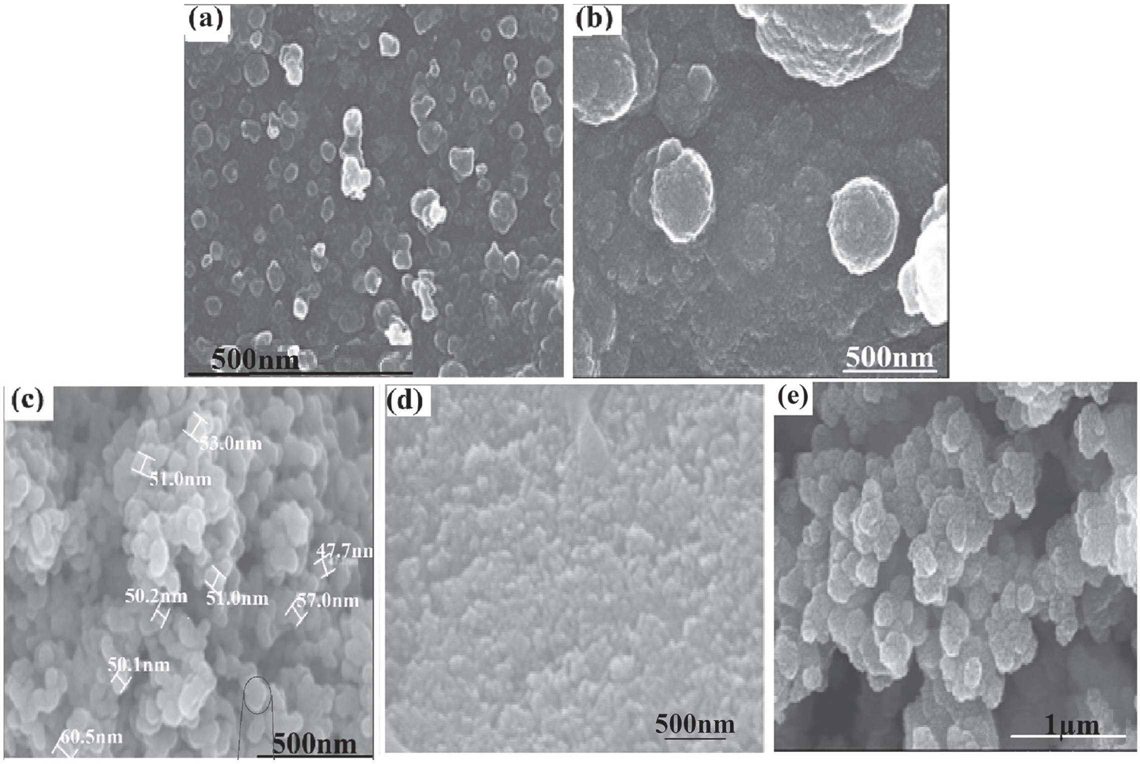

Figure 6. SEM micrographs of (a-b) Pristine PPy, (c) Ag_2S nanoparticles, (d) CdS nanoparticles, and (e) PPy/(Ag_2S:CdS) hybrid nanocomposites.

The formation of AC3 nanocomposites can be confirmed from Figure 7 (b) showing peaks of Ag, Cd and S as well as C and N. However, it can be seen from the spectrum, peaks of Ag (2.39 wt%), Cd (0.34 wt%) and S (0.55 wt%) were high, which indicates that the composition of PPy nanocomposites was more dominated by Ag_2S nanoparticles than CdS nanoparticles.

3.6. *Electrical behavior*

The electrical conductivity of PPy was recorded as 1.9×10^{-3} S/cm with ohmic behavior[7,10] (Figure 8). The conductivity of the PPy hybrid nanocomposites was observed to be varied with the addition of different ratios of (Ag_2S-CdS) nanoparticles. The current-voltage (I-V) characteristics of the PPy/(Ag_2S:CdS) hybrid nanocomposites showed a semiconducting behavior. The electrical

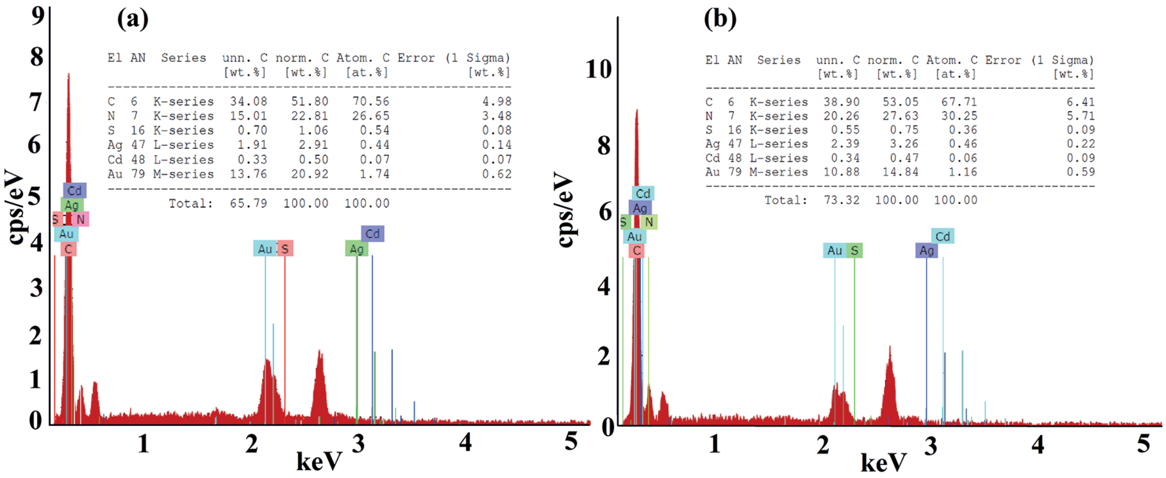

(a)

```
El AN  Series   unn. C norm. C Atom. C Error (1 Sigma)
                [wt.%]  [wt.%]  [at.%]          [wt.%]
-------------------------------------------------------
C  6  K-series  34.08   51.80   70.56             4.98
N  7  K-series  15.01   22.81   26.65             3.48
S  16 K-series   0.70    1.06    0.54             0.08
Ag 47 L-series   1.91    2.91    0.44             0.14
Cd 48 L-series   0.33    0.50    0.07             0.07
Au 79 M-series  13.76   20.92    1.74             0.62
-------------------------------------------------------
        Total:  65.79  100.00  100.00
```

(b)

```
El AN  Series   unn. C norm. C Atom. C Error (1 Sigma)
                [wt.%]  [wt.%]  [at.%]          [wt.%]
-------------------------------------------------------
C  6  K-series  38.90   53.05   67.71             6.41
N  7  K-series  20.26   27.63   30.25             5.71
S  16 K-series   0.55    0.75    0.36             0.09
Ag 47 L-series   2.39    3.26    0.46             0.22
Cd 48 L-series   0.34    0.47    0.06             0.09
Au 79 M-series  10.88   14.84    1.16             0.59
-------------------------------------------------------
        Total:  73.32  100.00  100.00
```

Figure 7. EDX of two PPy nanocomposites having ratio of (a) 1:2 and (b) 2:1 for Ag_2S:CdS hybrid of nanoparticles.

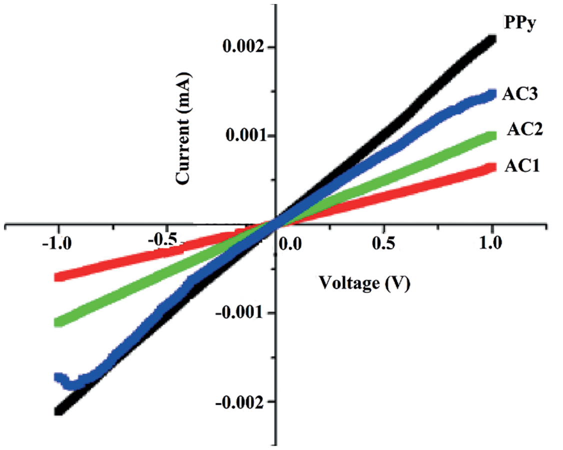

Figure 8. Current-voltage (I-V) characteristics of PPy and PPy/(Ag_2S-CdS) hybrid nanocomposites.

conductivity of the PPy hybrid nanocomposites was observed to be decreasing with addition of Ag_2S:CdS nanoparticles owing to charge compensation by these nanoparticles. Interestingly, the nanocomposites exhibited a lower conductivity when the Ag_2S and CdS content were equal; but still CdS nanoparticles content increased the conductivity. The order of electrical conductivities was observed to be PPy > AC3 > AC2 > AC1. The result reveals that lower content of metal sulphide nanoparticles decreases the electrical conductivity of the PPy based hybrid nanocomposites, while higher content possibly increases the conductivity by forming a conducting channel within the hybrid nanocomposites. However, the drop in conductivity may also due to localization of charge in p-type PPy by n-type Ag_2S nanoparticles[7].

3.7. *Gas sensing performance*

Room temperature gas sensing studies were carried out for the detection of NH_3 and LPG gases using two point–probe gas sensing setup. PPy and its hybrid nanocomposites (i.e. AC1, AC2 and AC3) as gas sensors were studied to determine their sensitivity and selectivity to specific gases at room temperature, and also to understand the underlying mechanism. A drop in current was observed with respect to the time when the samples were exposed to NH_3 gas (Figure 9 (a)). The corresponding response graph (Figure 9 (b)) shows an increase in gas response with respect to time when exposed to NH_3 gas. After an initial increase, the response curve shows no change which indicates saturation of the sensor surface by the analytes. As it has been discussed in our previous work[7], when a p-type semiconductor such as PPy is exposed to a reducing gas such as NH_3 there is a drop in charge concentration resulting from the donation of lone pairs of electrons of NH_3 to the PPy leading to a sudden rise in resistance. The gas response data are presented in Table 1. The AC1 nanocomposites show the maximum gas sensing response factor of 1.0 for the detection of 500 ppm NH_3 gas. For the same concentration, the response factors of AC2 and AC3 were recorded as 0.5 and 0.6, respectively. A decrease in response factor was observed with increasing the content of metal sulphide nanoparticles in the PPy matrix. This could be a result of charge compensation by the nanoparticles when present in higher content that renders the sensor incapable of accepting electrons from NH_3 gas. Therefore, the response of the sensor decreased with increase in nanoparticles content. Moreover, the most of the PPy based hybrid nanocomposites sensors exhibited a response time of ~ 20 s.

The change in response of the sensor with respect to variation in gas concentration was also studied. Figure 10 (a) shows that increasing the NH_3 gas concentration increases the response of the sensor. This can be well explained by the fact that incorporating the nanoparticles leads to increase in the surface roughness, which in turn facilitates adsorption of gas molecules easily. Higher the number of adsorbed gas molecules, higher would be the change in sensor's resistance due to the accepting electrons from NH_3 gas. This is in contrast with the

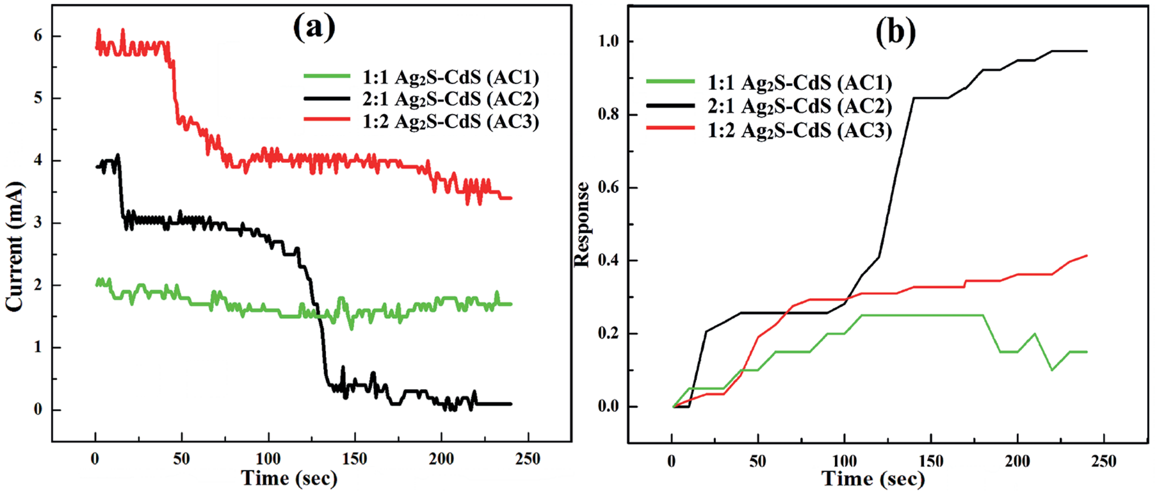

Figure 9. Various PPy/(Ag_2S-CdS) hybrid nanocomposites showing (a) Drop in current and (b) change in response factor with respect to time.

Table 1. Response factor values for sensing different concentration of NH_3 by PPy/(Ag_2S:CdS) hybrid nanocomposites.

PPy nanocomposites	Response factor value towards different concentration of NH_3 gas			Response Time (sec)
Ratio and code	100 ppm	250 ppm	500 ppm	
1:1 Ag_2S-CdS (AC1)	0.65	0.97	1.0	
2:1 Ag_2S-CdS (AC2)	0.33	0.38	0.5	20
1:2 Ag_2S-CdS (AC3)	0.25	0.56	0.6	

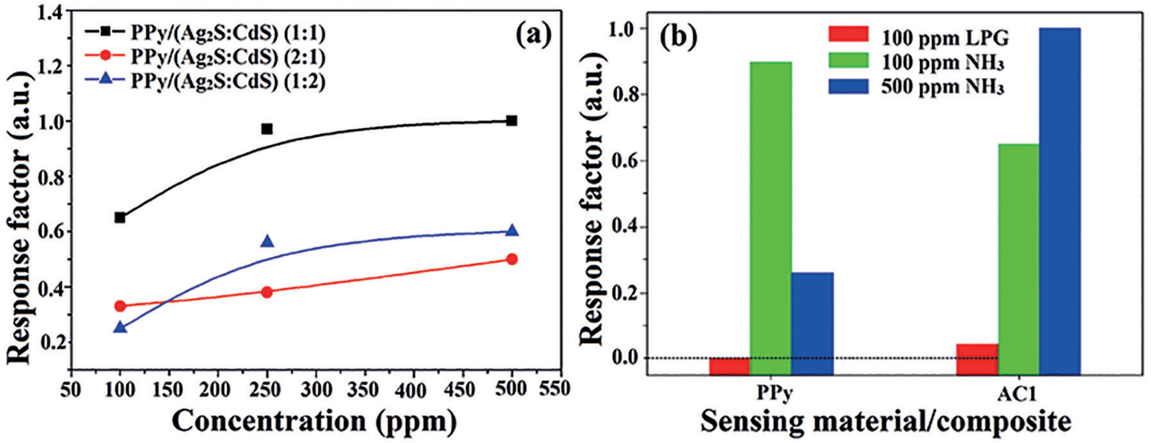

Figure 10. (a) Response factor vs concentration graph of PPy/(Ag_2S:CdS) hybrid nanocomposites towards NH_3 gas sensing; (b) Response factor and selectivity of PPy and PPy/(Ag_2S:CdS) (1:1) hybrid nanocomposites.

results observed for PPy (Table 2). In case of PPy, the sensor response decreased with increase in gas concentration due to saturation of the PPy surface with NH_3 gas, which was otherwise prevented in the nanocomposites by adding the metal sulphide nanoparticles. When pure PPy doped with $FeCl_3$ was exposed to NH_3 gas, an increment in the current was observed. During an oxidative polymerization for the preparation of PPy, the Cl^- ion is incorporated as counter ion to maintain its electro neutrality. Usually partial oxidation state (up to + 0.33) is produced in the process. In addition, it can be said that some amount of ions may remain within the PPy in the Fe^{2+} state. Thus, there is a possibility that higher oxidation state can be induced in the interaction with NH_3 gas molecules. In such a situation the higher charge on cations may lead to increase in current. The response of PPy and its all hybrid nanocomposites was also studied against LPG at room temperature. But they exhibited good sensitivity towards NH_3 gas, their response to LPG was found to be negligible for detection of 100 ppm of respective gases. Figure 10 (b) presents the gas response and selectivity of PPy and its hybrid nanocomposites towards detection of

Table 2. Response factor values for sensing LPG and ammonia gas by PPy.

Concentration (ppm)	Sensing factor	
	LPG	Ammonia
100	0.0	0.90
250	0.2	0.22
500	0.2	0.26

100 ppm of both LPG and NH_3. It can be clearly seen (Table 2) that PPy and its nanocomposite based sensors are selective towards detection of ammonia as compared to LPG at higher concentration (250 and 500 ppm) also. Therefore, not only the nanoparticles aided in a better sensing behavior, but also induced selectivity into the PPy nanocomposites.

4. Conclusions

Both Ag_2S and CdS nanoparticles were mixed in different ratios and incorporated into PPy matrix by ultrasound assisted *in-situ* polymerization for the preparation of PPy/(Ag_2S:CdS) hybrid nanocomposites. PPy and its hybrid nanocomposites were characterized using FTIR and UV-visible spectra, XRD and FESEM. Size of both nanoparticles of Ag_2S (40-65 nm) and CdS (60-100 nm) were observed at nanoscale, while the PPy showed globular and porous structures. The (I-V) characteristics revealed a semiconducting behavior of the resulting PPy hybrid nanocomposites. The gas sensing ability of the nanocomposite sensors at room temperature was determined using NH_3 gas. The sensing study underlines three important findings: (i) A low nanoparticle content aids in enhancing the sensitivity of the PPy/(Ag_2S:CdS) hybrid nanocomposite based sensors. At higher nanoparticles content the sensor loses its sensitivity either through the agglomeration of nanoparticles or by charge compensation by the nanoparticles. (ii) Unlike with PPy sensor, a gas response of the PPy/(Ag_2S:CdS) hybrid nanocomposite sensors increases with increase in gas concentration. This is possibly due to the increase in surface roughness, which facilitates adsorption of gas molecules on the sensor surface. (iii) Finally, the metal sulphide nanoparticles do not only impinge upon the sensor's sensitivity but also on its selectivity towards an analyte. The PPy/(Ag_2S-CdS) hybrid nanocomposites were found to be more selective towards NH_3 gas than LPG. Hence, metal sulphide nanoparticles provide a possibility to improve the existing CP based sensors in terms of their gas sensing performance.

5. Acknowledgment

Authors are thankful to University Grants Commission, New Delhi, Government of India for providing financial assistance under One Time Grant (UGC-BSR project no.: F.4-10/2010, dated 20 Sept., 2011) to carry out this research work.

6. References

1. Shimpi NG, Hansora DP, Yadav R, Mishra S. Performance of hybrid nanostructured conductive cotton threads as LPG sensor at ambient temperature: preparation and analysis. *RSC Advances.* 2015;5(120):99253-99269.

2. Shimpi NG, Mishra S, Hansora DP, Savdekar U, inventors; North Maharashtra University, assignee. An apparatus for continuous synthesis of carbon nano materials and a process for the same. Indian Patent 3179/MUM/2013. 2013 Oct 25. [cited 2016 Jul 11]. Available from: http://ipindia.nic.in/ipr/patent/journal_archieve/journal_2013/pat_arch_102013/official_journal_25102013_part_i.pdf

3. Hansora DP, Shimpi NG, Mishra S. Graphite to Graphene via Graphene Oxide: An Overview on Synthesis, Properties, and Applications. *The Journal of the Minerals, Metals & Materials Society.* 2015;67(12):2855-2868.

4. Shimpi NG, Mali AD, Hansora DP, Mishra S. Synthesis and Surface Modification of Calcium Carbonate Nanoparticles Using Ultrasound Cavitation Technique. *Nanoscience and Nanoengineering.* 2015;3(1):8-12.

5. Sen T, Shimpi NG, Mishra S, Sharma R. Polyaniline/γ-Fe_2O_3 nanocomposite for room temperature LPG sensing. *Sensors and Actuators B: Chemical.* 2014;190:120-126.

6. Mishra S, Ghanshyama C, Ram N, Bajpai RP, Bedi RK. Detection mechanism of metal oxide gas sensor under UV radiation. *Sensors and Actuators B: Chemical.* 2004;97(2-3):387-390.

7. Yeole B, Sen T, Hansora DP, Mishra S. Effect of electrical properties on gas sensitivity of polypyrrole/cds nanocomposites. *Journal of Applied Polymer Science.* 2015;132(32):42379.

8. Adhikari B, Majumdar S. Polymers in sensor applications. *Progress in Polymer Science.* 2004;29(7):699-766.

9. Persaud KC. Polymers for chemical sensing. *Materials Today.* 2005;8(4):38-44.

10. Lu Y, Shi G, Li C, Liang Y. Thin polypyrrole films prepared by chemical oxidative polymerization. *Journal of Applied Polymer Science.* 1998;70(11):2169-2172.

11. Mishra S, Shimpi NG, Sen T. The effect of PEG encapsulated silver nanoparticles on the thermal and electrical property of sonochemically synthesized polyaniline/silver nanocomposite. *Journal of Polymer Research.* 2013;20:49.

12. Chougule MA, Dalavi DS, Mali S, Patil PS, Moholkar AV, Agawane GL, et al. Novel method for fabrication of room temperature polypyrrole–ZnO nanocomposite NO_2 sensor *Measurement.* 2012;45:1989-1996.

13. Shumaila GB, Lakshmi VS, Alam M, Siddiqui AM, Zulfequar M, Husain M. Synthesis and characterization of Se doped polyaniline. *Current Applied Physics.* 2011;11(2):217-222.

14. Sen T, Shimpi NG, Mishra S. Room temperature CO sensing by polyaniline/Co_3O_4 nanocomposite. *Journal of Applied Polymer Science*. DOI: 10.1002/app.44115

15. Sharma S, Madou M. A new approach to gas sensing with nanotechnology. *Philosophical Transactions of the Royal Society A. Mathematical, Physical and Engineering Sciences*. 2012;370(1967):2448-2473.

16. Rana VK, Akhtar S, Chatterjee S, Mishra S, Singh RP, Ha CS. Chitosan and Chitosan-co-Poly(ε-caprolactone) Grafted Multiwalled Carbon Nanotube Transducers for Vapor Sensing. *Journal of Nanoscience and Nanotechnology.* 2014;14(3):2425-2435.

17. Lu G, Xu J, Sun J, Yu Y, Zhang Y, Liu F. UV-enhanced room temperature NO_2 sensor using ZnO nanorods modified with SnO_2 nanoparticles. *Sensors and Actuators B: Chemical.* 2012;162(1):82-88.

18. Chaudhari P and Mishra S, Effect of CuO as a dopant in TiO_2 on ammonia and hydrogen sulphide sensing at room temperature, *Measurement*, 2016; 90: 468-474.

19. Gupta N, Sharma S, Mir IA, Kumar D. Advances in sensors based on conducting polymers. *Journal of Scientific and Industrial Research.* 2006;65(7):549-557.

20. Cui S, Pu H, Mattson EC, Lu G, Mao S, Weinert M, et al. Ag nanocrystal as a promoter for carbon nanotube-based room-temperature gas sensors. *Nanoscale.* 2012;4(19):5887-5894.

21. Shen Y, Wan M. Soluble conductive polypyrrole synthesized by *in situ* doping with β-naphthalene sulphonic acid. *Journal of Polymer Science Part A: Polymer Chemistry.* 1997;35(17):3689-3695.

22. Lu X, Mao H, Zhang W. Fabrication of core-shell Fe3O4/ polypyrrole and hollow polypyrrole microspheres. *Polymer Composites.* 2009;30(6):847-854.

23. King RCY, Boussoualem M, Roussel F. Spectroscopic and electrical properties of 3-alkyl pyrrole–pyrrole copolymers. *Polymer.* 2007;48(1):4047-4054.

24. Prabhu RR, Khadar MA. Characterization of chemically synthesized CdS nanoparticles. *Pramana Journal of Physics.* 2005;65(5):801-807.

25. Joshi A, Gangal SA, Gupta SK. Ammonia sensing properties of polypyrrole thin films at room temperature. *Sensors and Actuators B: Chemical.* 2011;156(2):938-942.

26. Tang H, Yan M, Zhang H, Li S, Ma X, Wang M, et al. A selective NH_3 gas sensor based on Fe_2O_3–ZnO nanocomposites at room temperature. *Sensors and Actuators B: Chemical.* 2006;114(2):910-915.

27. Mani GK, Rayappan JBB. A highly selective room temperature ammonia sensor using spray deposited zinc oxide thin film. *Sensors and Actuators B: Chemical.* 2013;183:459-466.

28. Nguyen LQ, Phan PQ, Duong HN, Nguyen CD, Nguyen LH. Enhancement of NH3 Gas Sensitivity at Room Temperature by Carbon Nanotube-Based Sensor Coated with Co Nanoparticles. *Sensors.* 2013;13(2):1762-1754.

29. Han G, Shi G. Porous polypyrrole/polymethylmethacrylate composite film prepared by vapor deposition polymerization of pyrrole and its application for ammonia detection. *Thin Solid Films.* 2007;515(17):6986-6991.